Level and line broadening for Thomas-Fermi atoms at finite temperature

D. Shalitin, J. Stein, and Akiva Ron
Racah Institute of Physics, The Hebrew University of Jerusalem, Jerusalem 91904, Israel
and Department of Physics and Astronomy, University of Pittsburgh, Pittsburgh, Pennsylvania 15260
(Received 19 September 1983)

We present a new approach for estimating line broadening. It relies upon the Thomas-Fermi model at finite temperature and on the assumption of local thermodynamic equilibrium. This method can predict general features without requiring detailed computations of specific effects, usually encountered in accurate calculations of line broadening. Obviously, no very precise results can be expected from our nonspecific approach, but rather plausible estimates of the general features can be obtained with only modest effort. Results for a Hf plasma are presented and compared with experimental observations.

I. INTRODUCTION

The phenomenon of line broadening is well known[1] and so are its applications (e.g., computation of opacities[2]). The standard treatment involves explicit calculation of those effects which are believed to be the major contributors to line broadening (e.g., Stark effect). We present here a different approach, which is capable of estimating line broadening although it ignores some of the finer details. It turns out that when this method is valid (e.g., for high densities) the finer details which were neglected have hardly any influence on the results.

Our method is statistical in nature and it does not consider any specific effects that should have otherwise been taken into account explicitly. In this way we avoid some of the obstacles encountered in the standard methods: We do not have to worry about which of the many possible processes need to be included for the particular case under consideration, and we do not face the difficulties which usually occur when attempting to calculate these effects with sufficient accuracy. Since we employ single-particle lines of an average atom in the framework of the Thomas-Fermi (TF) model, we also avoid the computation of a huge number of terms and configurations as explained further on.

The treatment of a many-electron atom is a rather complicated problem, even for the case of an isolated atom in its ground state. Nevertheless this problem has been approximately solved by several methods which generally yield quite satisfactory results. It was shown that the simple TF model is exact in the limit of large Z.[3] In the isolated-atom case and finite Z, simple single-particle models, such as some versions of the TF model, already give good level energies for the ground states of atoms and positive ions.[4] The lines (transition energies) are sharp except for their natural width. Now in the relativistic treatment spin-orbit interaction splits the allowed single-particle lines into doublets whose components are usually very close to each other. In a real many-electron atom, the electrostatic and magnetic interactions further split each line into an array of very narrowly spaced lines.

When the atoms are embedded in a plasma this picture changes gradually with increasing temperature and density. The possibility of excitation, especially in a hot plasma, gives rise to many different states of ionization of the atoms and for each ion many possible initial (final) configurations (not just the ground state). Also the mutual interactions between the radiating atoms and surrounding atoms, ions or free electrons cause the sharp levels to spread into bands. This happens because electrons in different atoms but in the same nominal level (n,l,j) "see" different time-dependent electrostatic potentials which vary from atom to atom. The discrete splittings and continuous spreadings of the levels cause the same phenomena in lines. The transition between two given configurations gives rise to a number of lines. We refer to the collection of all such allowed lines as an "array of lines." We call a "cluster of lines" the collection of all allowed lines between two single-electron states (subshells). Obviously a cluster includes a number of arrays stemming from various possible configurations and states of ionization and excited states. Each line is further continuously broadened by various mechanisms, like the Doppler effect (movement of the ion) and the shortening of the lifetimes of the levels due to collisions. Evidently some of these broadened lines can merge together to form still broader lines.

In this paper we refer to the joint effect of "discrete splitting" and "continuous broadening" as "broadening." It is our aim to estimate broadenings caused by splitting of ionization and excitation states, which is in fact a computation of broadening of lines originating from transitions between different single-electron levels. Therefore, we assume that splittings within configurations are small and can be ignored. In this picture arrays of lines belonging to the same cluster merge together. The merging phenomenon has been observed experimentally[5] where in some cases one sees almost smooth curves rather than discrete peaks. If, on the other hand, configurations are electrostatically split wider than splittings caused by the different states of ionization and excited states, then the present treatment is naturally less adequate.[6]

A straightforward computation which treats each of the possible configurations is of course very difficult to carry

out due to their enormous number. This is still true when local thermodynamic equilibrium (LTE) is assumed, as we do in this work. (The LTE assumption is certainly justified for sufficiently dense plasmas and can still be adequate for our purpose when the deviations from LTE are not too large.) We choose to treat this problem by starting from a description in terms of an "average atom." The average atom is a fictitious atom defined as having for each given density and temperature, an initial configuration which is determined by average, not necessarily integral, occupation numbers appropriate to the collection of atoms in the plasma. Starting with the narrow lines of this average atom as our zeroth approximation we compute the broadening of these lines (which represent a cluster) due to the deviations from the average values of occupation numbers. The main idea in our derivation is to exploit the statistical nature of a model of an average atom and calculate the statistical fluctuations around the average occupation numbers. These fluctuations cause changes in the electrostatic potential which in turn yield changes in level energies and thus cause line broadenings. The standard deviation of these broadenings is believed to be a good estimate of the "typical" line broadening in a plasma of given temperature and density. However, we emphasize that we do not claim to calculate precise values for broadening with this procedure. We do however believe that this approach yields quite plausible estimates of the actual values with minimal effort.

In the next section we present a somewhat detailed derivation of our method, which we then apply to the TF model. The method can be extended to deal with other possible models. In fact results of binding energies and bound-free cross sections for various modified TF models have been already reported.[7] Since it was shown there that these results are hardly sensitive to the particular model chosen, we prefer to concentrate in this paper on the TF model solely. In the final section we compare our results with the experimental ones and discuss our method. In an Appendix we discuss a consistency test for the TF model.

II. DERIVATION OF STATICTICAL LINE BROADENING

As already stated our method is based upon the concept of an average atom for which one computes an average-atom potential. The one-electron Schrödinger equation (or Dirac equation which we actually used in this work) is solved in this average-atom potential. The energy levels and wave functions thus obtained do not in general correspond to any particular real atom or ion. However, assuming that the true potentials of the most probable configurations do not differ much from this average potential, one may regard the energy levels and wave functions as zero-order estimates, and use perturbation methods to obtain higher-order approximations for the energy levels. Models of average atoms at finite temperature already exist; the TF model was suggested quite long ago,[8,9] and also the Debye-Hückel-Thomas-Fermi (DHTF) model.[10] Level energies and other physical quantities based upon these models and some of their versions have been published.[7] As one example of non-TF average atom models, we mention Rozsnyai's Hartree-Fock model.[11] It turns out that the simple TF model seems especially suitable for our approach to this problem. It is true that some of the more elaborate versions of the TF model (Fermi-Amaldi,[12] Thomas-Fermi-Dirac[13] and their modifications[4]) can yield better results for zero-temperature level energies. However, as already stated, the magnitude of the differences among the results obtained from the different versions does not appear to justify at this time the extra effort involved in carrying through all other computations. In this finite temperature and density case we are presently interested more in general features than in high-precision computations. We follow Latter's derivation[9] of extending the TF model to finite temperature and density for its simplicity. We consider a one-component plasma in which each atomic nucleus is placed in a sphere the volume of which is $1/\rho$ (where ρ is the atomic density) and its radius is r_0. We assume that the electrons are in thermal equilibrium with a heat reservoir of temperature $T \equiv 1/k\beta$, where k is Boltzmann's constant, and with an electron reservoir having a chemical potential μ (or in the language of solid-state physics a Fermi energy μ). In this model the electrons come in and out of the fixed volume of the atom. Thus the atom is electrically neutral on the average, but not at any given moment. We prefer this picture to the confined-atom picture in which the atom is always neutral, because the former is more physically sound, and, besides, it makes the treatment of fluctuations easier.

One can assume that at each point in configuration space there exists an average electrostatic potential $V^a(\vec{r})$ due to the joint effects of the nucleus and all Z electrons (the superscript a denotes an average value). According to Fermi-Dirac statistics the average density in phase space of a macroscopic system of noninteracting particles is

$$\rho_e^a(\vec{r},\vec{p}) = \frac{2}{(2\pi\hbar)^3} \frac{1}{\exp\{[-eV^a(\vec{r}) + p^2/2m - \mu]/kT\} + 1} . \tag{1}$$

The average density of particles in configuration space is

$$\begin{aligned} \rho_e^a(\vec{r}) &= \int d^3p\, \rho_e^a(\vec{r},\vec{p}) \\ &= \frac{2^{1/2}(mkT)^{3/2}}{\pi^2\hbar^3} I_{1/2}([\mu + eV^a(\vec{r})]/kT) , \end{aligned} \tag{2}$$

where $I_n(\eta)$ are the Fermi-Dirac functions:

$$I_n(\eta) = \int_0^\infty \frac{y^n dy}{e^{y-\eta}+1} . \tag{3}$$

For $\eta \to \infty$ one gets $I_n \propto \eta^{n+1}$, and for $\eta \to -\infty$, $I_n(\eta) \propto e^\eta$.

A second relation between $\rho_e^a(\vec{r})$ and $V^a(\vec{r})$ is provided by Poisson's equation, which in the case of a point nucleus becomes

$$\nabla^2 V^a(\vec{r}) = 4\pi e \rho_e^a(\vec{r}) - 4\pi e Z \delta(\vec{r}) . \tag{4}$$

The solution of Eqs. (2) and (4), for the unknowns $\rho_e^a(\vec{r})$, $V^a(\vec{r})$, and μ, is unique if the two boundary conditions are fulfilled:

$$V^a(r_0)=0 \tag{5a}$$

which is the natural choice of zero potential energy, and

$$\int_0^{r_0} \rho_e^a(\vec{r})d^3r=Z \tag{5b}$$

which is the constraint on the average charge density. The second of these boundary conditions implies $[\partial V^a(r)/\partial r]\,|_{r=r_0}=0$. Since the problem is spherically symmetric we will use r instead of $\vec{r}$ where possible. The singular part of Eq. (4) may be replaced by the additional boundary condition:

$$\lim_{r\to 0}[rV^a(r)]=Ze\ . \tag{5c}$$

Note that the chemical potential μ is a function of ρ and T. Therefore, our method of solution consists of iterations for different values of μ until our boundary conditions are fulfilled.

The potential $V^a(r)$, which in fact depends also on T and ρ can now be used as an average-atom potential to compute zero-order energy levels and wave functions, by solving the Schrödinger equation (or the Dirac equation). We get then a series of one-electron levels, $E_i^a(\rho,T)$, all associated with the same potential $V^a(r;\rho,T)$. The only quantum effect which we introduced in order to calculate the potential is the Fermi-Dirac statistics. Nevertheless it is instructive to see that there is in fact some consistency between the semiclassical $\rho_e^a(r), V^a(r)$ and the quantum energy levels and wave functions. This is discussed in the Appendix.

The width and shape of a level (in the sense that was described in the Introduction), due to fluctuations in the occupation numbers of the electrons of different atoms, can be estimated as follows: Suppose that the local density in phase space for a particular atom is

$$\rho_e(\vec{r},\vec{p})=\rho_e^a(r,p)+\delta\rho_e(\vec{r},\vec{p})\ , \tag{6}$$

where $\rho_e^a(r,p)$ is the electron density in the average atom, assumed to be the average of $\rho_e(\vec{r},\vec{p})$ over all atoms. The electrostatic potential at any given point $\vec{r}'$ is

$$V(\vec{r}')=\frac{Ze}{r'}-\int\frac{d^3r\,d^3p\,e\rho_e(\vec{r},\vec{p})}{|\vec{r}-\vec{r}'|}$$

$$=\frac{Ze}{r'}+V_e^a(r')+\delta V_e(\vec{r}') \tag{7}$$

where

$$\delta V_e(\vec{r}')=-e\int\frac{d^3r\,\delta\rho_e(\vec{r})}{|\vec{r}-\vec{r}'|} \tag{8}$$

and

$$\delta\rho_e(\vec{r})=\int d^3p\,\delta\rho_e(\vec{r},\vec{p})\ . \tag{9}$$

If most deviations from the average are small (as is the case in a macroscopic system) then most deviations in the values of the binding energies will also be small. Therefore, first-order perturbation theory may be used for the computation of these deviations. The effect of such a fluctuation $\delta\rho_e(\vec{r})$ on the energy level E_i is

$$\delta E_i=E_i-E_i^a$$

$$=-\int|\psi_i^a(\vec{r}')|^2e\delta V_e(\vec{r}')d^3r'$$

$$=\int d^3r\,d^3r'e^2\frac{\delta\rho_e(\vec{r})\,|\psi_i^a(\vec{r}')|^2}{|\vec{r}-\vec{r}'|}$$

$$=-e\int v_i(\vec{r})\delta\rho_e(\vec{r})d^3r\ , \tag{10}$$

where

$$v_i(\vec{r})=-e\int d^3r'\frac{|\psi_i^a(\vec{r}')|^2}{|r-r'|} \tag{11}$$

is the electrostatic potential induced by the electron in level i described by a wave function $\psi_i^a(\vec{r})$ as calculated in the average-atom potential. In order to simplify the calculation we approximate the potential by the first term of its multipole expansion. Thus Eq. (11) is replaced by

$$v_i(r)=-e\int d^3r'\frac{|\psi_i^a(\vec{r}')|^2}{\max(r,r')}\ . \tag{11'}$$

We shall define ΔE_i as the root mean square of (δE_i) averaged over all atoms:

$$(\Delta E_i)^2=\langle(\delta E_i)^2\rangle=e^2\left\langle\left[\int v_i(r)\delta\rho_e(\vec{r})d^3r\right]^2\right\rangle$$

$$=e^2\left\langle\int v_i(r)v_i(r')\delta\rho_e(\vec{r})\delta\rho_e(\vec{r}')d^3r\,d^3r'\right\rangle$$

$$=e^2\int v_i(r)v_i(r')\langle\delta\rho_e(\vec{r})\delta\rho_e(\vec{r}')\rangle d^3r\,d^3r'\ . \tag{12}$$

We may also estimate the correlation function $\langle\delta\rho(\vec{r})\delta\rho(\vec{r}')\rangle$ within the TF description. For this purpose we will further assume that deviations at different points in phase space are uncorrelated. The assumption is valid for noninteracting fermions in a potential, a description which was fundamental in obtaining Eq. (1).

Consider volume elements in phase space, labeled by some index j. The size of the jth volume element is $\frac{1}{2}(2\pi\hbar)^3\Omega_j$; Ω_j is the number of cells in the volume. [Each cell in phase space which contains at most one electron has a volume $\frac{1}{2}(2\pi\hbar)^3$; the factor $\frac{1}{2}$ is due to the two possible spin states.] The probability that N_j noninteracting particles having similar energies will occupy the Ω_j cells of the jth volume element is given by the binomial distribution

$$\binom{\Omega_j}{N_j}n_j^{N_j}(1-n_j)^{\Omega_j-N_j}\ , \tag{13}$$

where n_j is the probability that an electron occupies a cell in phase space. The average occupation of the jth volume element is then

$$\langle N_j\rangle=n_j\Omega_j \tag{14}$$

and the fluctuation δN_j from the average occupation may be written in terms of the fluctuation $\delta\rho_e$ of the electron density in phase space as

$$\delta N_j=\frac{(2\pi\hbar)^3}{2}\Omega_j\delta\rho_e(\vec{r}_j,\vec{p}_j)\ . \tag{15}$$

The correlation $\langle \delta N_k \delta N_j \rangle$ between a fluctuation δN_k in the number of particles in cell k and a simultaneous fluctuation δN_j in a different cell j is given by

$$\langle \delta N_k \delta N_j \rangle = \Omega_j n_j (1-n_j)\delta_{jk} \ . \tag{16}$$

[Remember that we have assumed that fluctuations at different points in phase space are uncorrelated, resulting in the Kronecker delta. For $j=k$ we use the result for the variance $\langle N_j^2 \rangle - \langle N_j \rangle^2 \equiv \langle (\delta N_j)^2 \rangle = n_j(1-n_j)\Omega_j$.]

Now we also have that

$$n_j = \frac{1}{\exp[(E_j-\mu)/kT]+1} \ , \tag{17}$$

where

$$E_j = E(r_j,p_j) = p_j^2/2m - eV(r_j) \tag{18}$$

is the energy of a classical electron at a point $(\vec{r}_j, \vec{p}_j)$. Assuming these expressions remain valid in the limit $\frac{1}{2}\Omega(2\pi\hbar)^3 \to 0$, and taking into account Eq. (15) and

$$\delta(\vec{p}_i - \vec{p}_j)\delta(\vec{r}_i - \vec{r}_j) = \lim_{\Omega_i h^3 \to 0} \frac{\delta_{ij}}{\frac{1}{2}\Omega_i h^3} \tag{19}$$

yield

$$\langle \delta\rho_e(\vec{r},\vec{p})\delta\rho_e(\vec{r}',\vec{p}') \rangle = \delta(\vec{r}-\vec{r}')\delta(\vec{p}-\vec{p}')\frac{2}{(2\pi\hbar)^3}\frac{\exp\{[E(r,p)-\mu]/kT\}}{(\exp\{[E(r,p)-\mu]/kT\}+1)^2} \ , \tag{20}$$

and therefore

$$\begin{aligned}\langle \delta\rho_e(\vec{r})\delta\rho_e(\vec{r}') \rangle &= \frac{\delta(\vec{r}-\vec{r}')}{4\pi^3\hbar^3}\int d^3p \frac{\exp[(E-\mu)/kT]}{\{\exp[(E-\mu)/kT]+1\}^2} \\ &= \frac{(2mkT)^{3/2}}{4\pi^2\hbar^3} I_{-1/2}([\mu+eV^a(r)]/kT)\delta(\vec{r}-\vec{r}') \ .\end{aligned} \tag{21}$$

Hence Eqs. (12) and (21) yield

$$(\Delta E_i)^2 = \frac{(2mkT)^{3/2}}{4\pi^2\hbar^3} e^2 \int [v_i(r)]^2 I_{-1/2}([\mu+eV^a(r)]/kT) d^3r \ . \tag{22}$$

This is our expression for the broadening of an energy level, due to thermal fluctuations in the occupation numbers in phase space, within the TF model. [Note that by Eq. (3) $(\Delta E_i)^2 \propto T$ for $T \to 0$, and for $T \to \infty$, $\Delta E_i \to$ const.]

We follow the derivation of Eq. (22) in order to calculate the width of a transition line between levels having energies E_i and E_j. We start by utilizing Eq. (10) and define

$$\delta E_{ij} = \delta E_i - \delta E_j = -e \int [v_i(r) - v_j(r)]\delta\rho_e(\vec{r}) d^3r \ . \tag{23}$$

Following a similar procedure finally yields the width of a transition line:

$$(\Delta E_{ij})^2 = \langle (\delta E_{ij})^2 \rangle = \frac{(2mkT)^{3/2}}{4\pi^2\hbar^3} e^2 \int [v_i(r) - v_j(r)]^2 I_{-1/2}([\mu+eV^a(r)]/kT) d^3r \ . \tag{24}$$

The fluctuations which we described cause level and also transition energies to appear as bands rather than sharp values. Therefore, we have to refine the treatment of transition probabilities which are defined for sharp values and introduce cross sections. The spontaneous emission probability $A_{\mu\to\mu'}$ for a very narrow transition between states μ and μ' is given, in the nonrelativistic dipole approximation, by the expression

$$A_{\mu\mu'} = \frac{4\alpha\omega^3}{3e^2} |\langle \mu | \vec{r} | \mu' \rangle|^2 \ , \tag{25}$$

where $\alpha = e^2/\hbar c = 1/137$. If $\sigma_{\mu'\to\mu}(\hbar\omega)$ is the cross section for photoabsorption of a very narrow transition, then

$$\int \sigma_{\mu'\to\mu}(\hbar\omega) d(\hbar\omega) = \frac{g_\mu \pi^2 c^2 \hbar^3}{g_{\mu'}(\hbar\bar{\omega})^2} \bar{A}_{\mu\to\mu'} \ . \tag{26}$$

$\bar{A}_{\mu\to\mu'}$ is an average (over a group of nearly degenerate states) of the transition probability for an atom in initial state μ to a final state μ'. The initial (final) state μ (μ') is any of the g_μ ($g_{\mu'}$) degenerate initial (final) states, and $\hbar\bar{\omega}$ is the average energy. In this presentation we have replaced the discrete line by a continuous one but kept $\int \sigma(\hbar\omega) d(\hbar\omega)$ constant. The shape of the line is Gaussian with a standard deviation of $\Delta E_{\mu\mu'}$ [see Eq. (24)]. The Gaussian shape is a necessary consequence of the assumption that the broadening is caused by many small but independent effects. Keeping $\int \sigma(\hbar\omega) d(\hbar\omega)$ constant (i.e., independent of the line shape) in deriving (26) is fully justified as long as $\Delta E \ll \hbar\omega$ and $\Delta E \ll |E_h|$, where E_h is the energy of the higher level of the two. However, we still use it also for wider lines, expecting that a more sophisticated treatment would change but slightly the final results.

III. RESULTS AND DISCUSSION

We illustrate our method by presenting a few emission spectra of Hf ($Z=72$) at temperatures $kT=300$ and 350

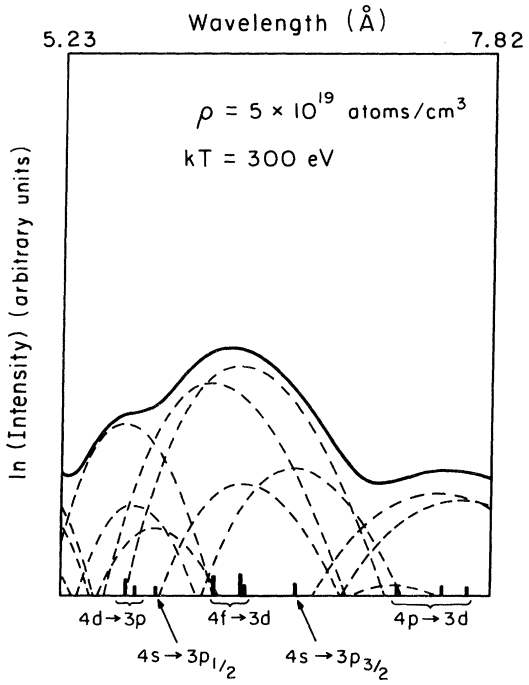

FIG. 1. Emission spectrum of a Hf plasma at temperature of $kT=300$ eV and density of $\rho=5\times10^{19}$ atoms/cm^3, according to the TF model is presented over the same wavelength range as in Ref. 14. Solid curve is the intensity of the spectrum. Dashed curves are the separate broadened lines. The short bars on the abscissa indicate the centers (location of the maxima) of the separate lines. (Note that some of the dashed curves have their centers outside the graph boundaries.) The central peak is due to the three $4f\rightarrow3d$ transitions, the left peak is due to the two $4d\rightarrow3p_{3/2}$ transitions, and the right peak (only partially shown) is due to the three $4p\rightarrow3d$ transitions. Some less prominent and hardly noticable lines are the two $4s\rightarrow3p$ transitions (on the two sides of the main peak). Relativistic wave functions in a nonrelativistic TF potential were used.

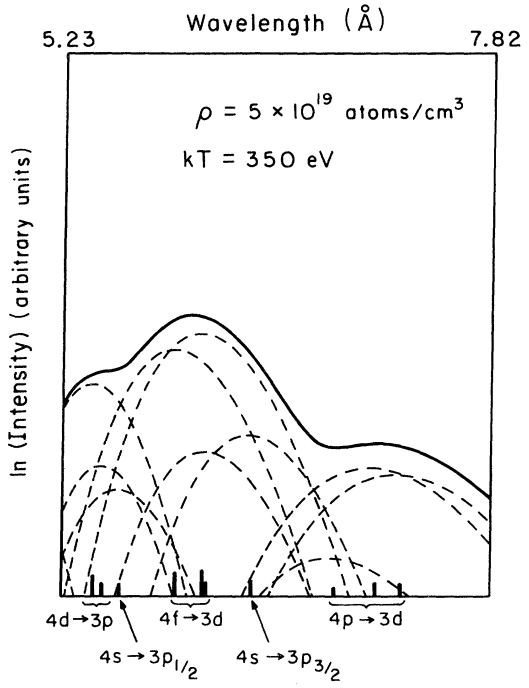

FIG. 2. Same as Fig. 1 but for $kT=350$ eV and $\rho=5\times10^{19}$ atoms/cm^3.

eV and at densities $\rho=5\times10^{19}$ and 5×10^{20} atoms/cm^3. We chose to present these spectra in order to simulate a previously measured and interpreted emission spectrum of a laser-produced plasma.[14] Figures 1–4 show our calculated TF spectra. These figures (and additional ones which are not presented here[15]) suggest that the major effect of temperature is to shift somewhat the location of the centers of the lines and hardly change their width. The density affects more the width (the higher the density the broader the line) and to a lesser degree it also shifts the spectrum. Figures 1 and 4, out of our four examples, bear resemblance to the experimental result (Fig. 1 of Ref. 14). In both graphs the general structure and locations of the "hills" are quite close to those of the experimental graph. In all cases the theoretical TF lines seem to be too wide. This may be explained by the continuous nature of the TF electron density versus the shell structure of electrons in real atoms. In many cases the freedom to fluctuate is far greater in a TF model than it is for an actual atom. In a planned subsequent paper we will take into account the discrete nature and shell structure of the electrons while calculating the fluctuations and their effects on the line (cluster) width.

In seeking a simple model which gives a reasonable description of the shapes of the prominent features (hills rather than sharper peaks) in spectra of plasmas (e.g., Refs. 5 and 14), we have restricted ourselves to average-atom models. In this paper we have presented a detailed

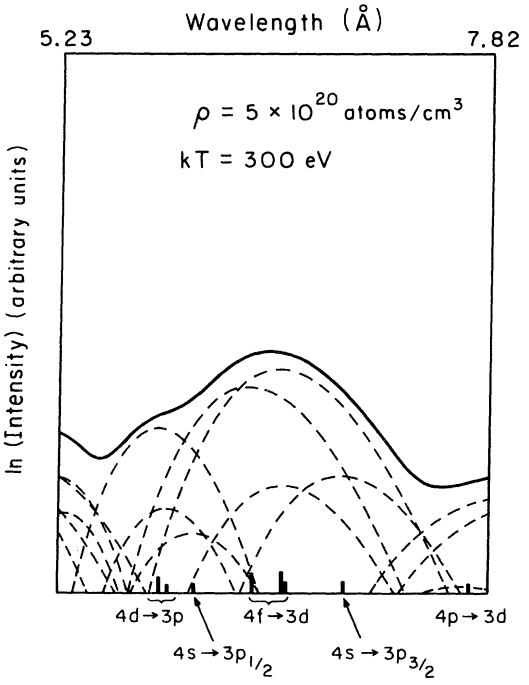

FIG. 3. Same as Fig. 1 but for $kT=300$ eV and $\rho=5\times10^{20}$ atoms/cm^3.

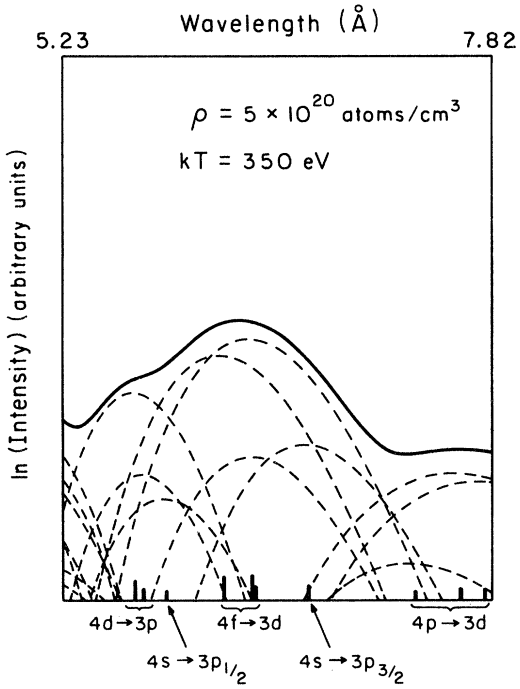

FIG. 4. Same as Fig. 1 but for $kT=350$ eV and $\rho=5\times10^{20}$ atoms/cm^3.

account for the TF model making a few plausible assumptions. Clearly we are assuming that by solving Eqs. (2)—(5) inside a sphere of radius r_0 we obtain a potential which does not differ much from the potentials of the most probable ionic configurations in the plasma. Then the subsequent first-order perturbation approach is justified.

The mere introduction of fluctuations in the number of electrons results in an "open-atom" model in which electrons are coming in and out of the sphere. Such a model which constrains only the average number of electrons is different from the confined-atom model (with impenetrable boundaries). However, we still find that the (time) average number of electrons in an atomic volume (and not the actual number for each individual fluctuation which is considered in calculating the width) is equal to Z. This open-atom model is equivalent to a confined atom with a fluctuating volume which we have not treated here explicitly, but is rather easy to accomplish. Another approach would be to keep the confined-atom model and artificially impose the constraint by appropriately normalizing the free-electron distribution. We examined this modification and found that it hardly changed the results. Another shortcoming of these models is that they ignore the penetration of neighbor ions into the atomic volume. This effect is better taken into account by the DHTF model. In the examples in which binding energies and bound-free cross sections were computed for the DHTF, TF, and some of its versions[7] it was found that differences between the various results were rather minor.

An additional and crucial assumption made here is that the actual line spectrum is sufficiently dense. Then, when each line is spread, by its natural width and by time-dependent mechanisms which cause continuous spreading (Doppler, Stark, collisions) the lines overlap and appear rather as continuous hilly features, as sometimes seen experimentally.[5,14] Our model gives the rough shape and location of these features but, of course, not the finer details of the individual lines. In a planned subsequent paper we intend to refine and extend the method beyond the TF model so that some of the details of the spectra will be revealed and the resemblance to experiment will improve.

ACKNOWLEDGMENT

It is a pleasure to thank Professor R. H. Pratt for fruitful discussions and a critical reading of the manuscript.

APPENDIX

We illustrate here the consistency of the TF approach with quantum mechanics, in the sense that the number of bound levels in the statistical framework agrees with the number of bound levels derived by quantum-mechanical calculations for the same statistical potential, and also in the agreement of the number of bound electrons calculated in the two methods.

Having found all the bound single-particle quantum levels in a given potential, one can plot $N_q(E)$, the number of bound quantum states not exceeding the negative energy E, as function of E. On the other hand, we can plot $N_s(E)$, the number of bound states according to the classical statistical procedure to which we add the assumption that there are two possible states in one cell of phase space volume $(2\pi\hbar)^3$. One gets then

$$N_s(E)=\frac{4}{\pi\hbar^3}\int_{-\infty}^{E}dE'\int_0^{r(E)}r^2m\{2m[E'+eV(r)]\}^{1/2}dr\ ,$$

where $eV[r(E)]=-E$ defines $r(E)$. Figure 5 shows these two curves computed for an iron plasma having temperature $kT=1$ keV and density $\rho=5\times10^{23}$ atoms/cm^3. The two curves show the resemblance which is expected when making statistical and quantum assumptions.

Another interesting comparison is between the electron populations derived by means of these two approaches. Let $P(E)$ be the average number of electrons occupying levels which have energies less than E. Then according to the quantum-mechanical approach

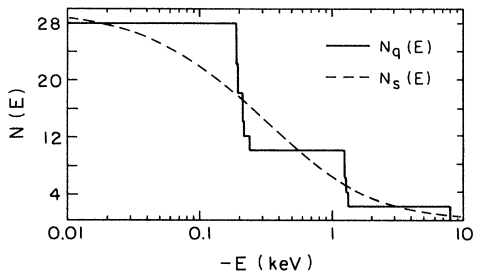

FIG. 5. Number of bound states in an iron plasma ($\rho=5\times10^{23}$ atoms/cm^3, $kT=1$ keV) according to a quantum calculation, N_q, and a statistical calculation, N_s, in a Thomas-Fermi potential.

$$P_q(E)=\sum_{E_j<E}\frac{g_j}{\exp[(E_j-\mu)/kT]+1},\quad E<0\,,$$

where g_j is the degeneracy of the level (usually equal to $2j+1$) and E_j is its energy. Analogously we define the average number of electrons occupying states according to the statistical model

$$P_s(E)=\frac{4}{\pi\hbar^3}\int_{-\infty}^{E}\frac{dE'}{\exp[(E'-\mu)/kT]+1}\times\int_0^{r(E')}r^2m\{2m[E'+eV(r)]\}^{1/2}dr\,.$$

Figure 6 shows these two curves computed for the same values of ρ and kT as in Fig. 5. Again we find a reasonable agreement. It is perhaps worth noting that for a pure Coulomb potential, Ze/r, one gets

$$N_s^{\text{Coul}}(E)=\frac{2}{3}\left[\frac{Ze^2}{2\hbar}\right]^3\left[\frac{2m}{-E}\right]^{3/2}=\tfrac{2}{3}n^3\,,$$

where $n=(m/-2E)^{1/2}(e^2Z/\hbar)$ is the analog of the principal quantum number. Then we have

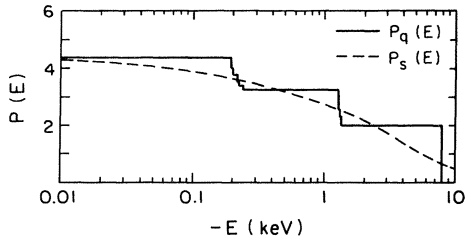

FIG. 6. Population of bound states in an iron plasma ($\rho=5\times10^{23}$ atoms/cm^3, $kT=1$ keV) according to a quantum calculation, P_q, and a statistical calculation, P_s, in a Thomas-Fermi potential.

$$N_q(E)=\tfrac{2}{3}n'^3\left[1+\frac{3}{2n'}+\frac{1}{2n'^2}\right]$$

$$=\tfrac{2}{3}(n'+\tfrac{1}{2})^3+O(n')\,,$$

where $n'=[n(E)]$ is the integral part of $n(E)$. Although such results are expected of any plausible model it is reassuring to find that they are indeed obtained in our case.

[1]Hans R. Griem, *Spectral Line Broadening by Plasmas* (Academic, New York, 1974), and references therein.
[2]S. Chandrasekhar, *Radiative Transfer* (Oxford University, New York, 1950).
[3]E. H. Lieb and B. Simon, Phys. Rev. Lett. 31, 681 (1973); E. H. Lieb, Rev. Mod. Phys. 53, 603 (1981).
[4]D. Shalitin, Phys. Rev. 140, A1857 (1965); 155, 20 (1967).
[5]Proceedings of the CECAM Workshop, Orsay, 1982; R. W. Lee and N. Spector (private communication).
[6]C. Bauche-Arnoult, J. Bauche, and M. Klapisch, Phys. Rev. A 20, 2424 (1979); M. Klapisch *et al., ibid.* 25, 2391 (1982). Figure 2 of the latter reference shows an example of arrays merging together to form a hill. We thank Dr. M. Klapisch for bringing this point to our attention.
[7]D. Shalitin, A. Ron, Y. Reiss, and R. H. Pratt, J. Quant. Spectrosc. Radiat. Transfer 27, 219 (1982).
[8]R. P. Feynman, N. Metropolis, and E. Teller, Phys. Rev. 75, 1561 (1949).
[9]R. Latter, Phys. Rev. 99, 1854 (1955).
[10]R. D. Cowan and J. G. Kirkwood, J. Chem. Phys. 29, 264 (1958).
[11]B. F. Rozsnyai, Phys. Rev. A 5, 1137 (1972).
[12]E. Fermi and E. Amaldi, Mem. Acc. Italia 6, 117 (1934).
[13]P. A. M. Dirac, Proc. Cambridge Philos. Soc. 26, 376 (1930).
[14]A. Zigler, H. Zmora, N. Spector, M. Klapisch, J. L. Schwob, and A. Bar-Shalom, J. Opt. Soc. Am. 70, 129 (1980).
[15]We thank Dr. D. Salzmann for advising us on the possible ranges of temperature and density we should try in order to simulate the experimental results.